Analysis of Polymers for Additive Manufacturing: Based Contact Pressure and Force Sensors

Tiziano Fapanni[1][a], Jacopo Agnelli[2][b], Raphael Rosa[3][c], Giuseppe Rosace[3][d],
Francesco Baldi[2][e] and Nicola Francesco Lopomo[4][f]

[1]Department of Information Engineering, University of Brescia, Brescia, Italy
[2]Department of Mechanical and Industrial Engineering, University of Brescia, Brescia, Italy
[3]Department of Engineering and Applied Science, University of Bergamo, Bergamo, Italy
[4]Department of Design, Politecnico di Milano, Milan, Italy

Keywords: Contact Pressure Sensors, Force Sensors, Additive Manufacturing.

Abstract: The rapid advancements in Industry 4.0 and wearable technology have heightened the demand for flexible, robust, and sensitive sensors that can be integrated into diverse applications. This work investigates the potential of various polymeric materials, processed through additive manufacturing techniques such as Fused Deposition Modeling (FDM) and Stereolithography (SLA), to act as transducers in contact pressure and force sensors. In this work, four possible polymeric materials were tested. Those materials were specifically selected to present both capacitive and piezoresistive transduction principles, aiming to develop flexible and highly sensitive sensors to pressure variations. In this frame, one of the key challenges is the hysteretic behavior typical of polymeric materials, which affects both mechanical (16.9 % on average) and electrical performance (20.7 % and 24.4% on average on capacitive and resistive devices, respectively). It must be underlined that significant variations were noted between the filled materials and the microstructured one, with the latter one being less stiff and able to withstand lower loads (up to 90 N) with an impressive 13-fold increase in sensitivity compared to thermoplastic polyurethane (TPU). This novel approach seems to pave the way for optimizable sensor performance in terms of sensitivity at low loads.

1 INTRODUCTION

Following to the Industry 4.0 paradigm, a new technological era has emerged, thanks to the integration of different digital tools such as Big Data, Internet of Things (IoT), Additive Manufacturing (AM) and Cloud Computing. These technologies enable a synergistic relationship between humans and Smart Objects (SOs), a set of interconnected devices that compose smart systems (Kortuem et al., 2010; Munirathinam, 2020). SOs are thus devices equipped with sensors, microcontrollers, and AI-based algorithms, that can monitor variations in physical parameters (*e.g.* temperature, humidity, mechanical deformations, etc.). The real-time collection, elaboration and transmission of this data allow for the creation of a digital tread approach that, thanks to advanced analytics, fosters new functionalities such as real-time monitoring, automation, and preventive maintenance in general, thus improving the possibilities of each device and their production process as well (Bianchini et al., 2024). The flexibility of SOs can be seen across a wide range of industries. For example, in sports, SOs can monitor athletes' health, suggest how to improve their performances, reduce the risk of injuries, and foster

[a] https://orcid.org/0000-0002-5164-6907
[b] https://orcid.org/0009-0003-8393-2654
[c] https://orcid.org/0000-0002-9744-9511
[d] https://orcid.org/0000-0003-0604-4453
[e] https://orcid.org/0000-0001-6174-4474
[f] https://orcid.org/0000-0002-5795-2606

engagement (Mendes et al., 2016). In industrial settings, SOs provide the possibility to enhance worker safety, as they can track physiological and environmental conditions, detecting critical changes such as temperature/humidity fluctuations or hazardous pollutants levels (Podgórski et al., 2017); these insights can help reduce accidents and improve overall workplace safety and the overall quality of the product (Borghetti et al., 2021; Saqlain et al., 2019). In many applications, one of the key parameters to be monitored is the contact pressure or the exchange force at the mechanical interfaces, whose measure requires custom sensors to be developed. These sensors can detect and measure pressure variations, which are vital for applications ranging from wearable devices to robotics. Over the years, a variety of pressure transducers have been explored, including piezoresistive, piezoelectric, capacitive, and optical (Laszczak et al., 2015; Mannsfeld et al., 2010; Pan et al., 2014; Persano et al., 2013; Ramuz et al., 2012; Sun et al., 2020). Among these, capacitive pressure sensors are particularly attractive due to their high sensitivity, excellent repeatability, low power consumption, and ability to function independently of temperature variations (Chortos et al., 2016). On the other hand, piezoresistive contact pressure sensors are often easy to produce and use, require low power consumption, and present a high sensitivity in the low-pressure range (Gao et al., 2019). Both those transduction principles can be explored and developed on flexible and complex geometries using additive manufacturing (AM). In fact, in recent years, AM has emerged as a leading technology for innovative fabrication and prototyping. Two of the most commonly employed AM techniques are Fused Deposition Modeling (FDM) and Stereolithography (SLA). These techniques allow for the creation of customized, complex geometries using a range of polymeric materials, making them highly suitable for the development of flexible and wearable pressure sensors (José Horst & De Almeida Vieira, 2018). In particular, FDM is a widely used 3D printing process that involves the layer-by-layer deposition of thermoplastic filament, to create a part both in automotive, aviation and space (Wawryniuk et al., 2024); this method is particularly useful for producing robust and flexible components. On the other hand, stereolithography (SLA) is a high-resolution additive manufacturing technique that uses ultraviolet (UV) light to cure photopolymer resins layer-by-layer (Afridi et al., 2024); this process allows for the creation of intricate and highly detailed structures. In the development of contact pressure sensors, SLA offers precision and flexibility, making

it a suitable choice for creating complex sensor geometries. Moreover, SLA can be used with various resins, including flexible materials, which are crucial for wearable applications. This research aimed to investigate various additive manufacturing polymers for the development of contact pressure sensors with potential applications in wearable devices, industrial settings, and robotics. By exploring the properties of different polymers and the advantages of both FDM and SLA techniques, this work aimed to develop highly customizable sensors that can adapt to the specific needs of each application. The sensors designed in this study are capacitive, meaning they rely on the ability to measure changes in capacitance when pressure is applied. In order to achieve resistive behavior, two materials were selected to explore their piezo-resistive capabilities. Moreover, a preliminary microstructured device was fabricated using the SLA resin to further enhance sensor performance, particularly at low load levels.

2 MATERIALS AND METHODS

2.1 Materials Selection

In this work, a set of different polymers were taken into account to provide different possibilities for contact pressure sensors. In order to explore both resistive and capacitive sensors, both conductive and dielectric materials were specifically selected. According to this idea, a flexible resin (SuperFlex Clear, 3DMaterials, Gyeonggi-do, Republic of Korea) for stereolithography (SLA) was selected and mixed with 1% of carbon black (CB) in order to obtain a resistive material; the CB loading was limited by its dark color which can block the UV light properly to properly sinter the resin itself. A second conductive material is a CB-loaded thermoplastic elastometer (TPE) provided by ALLOD (Burgbernheim, Germany) in the form of a slab. Moreover, a thermoplastic polyurethane (TPU) filament for fused deposition modelling (FDM) machines was employed. To further provide devices with reduced stiffness that can present good sensitivity at low loads, the SLA mentioned above resin was used out of the box to produce a set of microstructured devices; those devices are composed of a set of unitary cells that can be modeled in 3D as the combination of four 3D pyramidal structures (Fapanni et al., 2024).

2.2 Sample Preparation

Each material was prepared in 20 x 20 mm samples with a thickness ranging from 1.7 mm to 3 mm according to the different production techniques used. The samples produced with the superflex resin were produced using a stereolithographic printer Photon Mono M5s, by Anycubic. The devices in TPU were printed with an FDM printer, while the TPE slab was cut in shape using a laser cutter. Then, in order to provide easy electrical contact, copper tape was used to cover the two 20 x 20 mm samples completely. The tape was then shaped to provide a simple wiring line with a taper, to avoid sharp edges that could introduce undesired stray effects.

2.3 Sensor Electrical Model

From the electrical point of view, the devices can be seen as a two-pole composed of a capacitor and a resistor in parallel as shown in Figure 1.
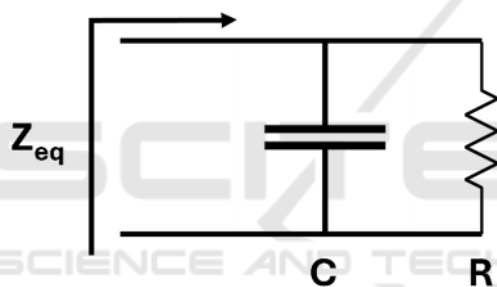

Figure 1: Electrical reference model for the DUTs.

Considering mainly capacitive devices, it is possible to consider the capacitance C proportional to the surface area A of the devices, the relative permittivity of the insulating layer ε_r and the vacuum permittivity ε_0, while it is inversely proportional to the device thickness, d, according to the relationship

$$C = (\varepsilon_0\ \varepsilon_r\ A)/d \qquad (1)$$

It is thus possible to modify the capacitance of the device, by changing either the thickness of the device (*e.g.* by applying a load to compress the device) or changing the relative permittivity of the device due to the applied load (Fapanni et al., 2024). On the other hand, for CB-loaded materials, the resistance is provided by creating an electrical path between the plates thanks to the conductive CB particles (El Hasnaoui et al., 2012). When the device is compressed, the internal disposition of the CB-particle network is modified, leading to variations in the resulting resistance (Oh et al., 2022).

2.4 Experimental Setup

In order to characterize the devices as contact pressure sensors, the experimental setup was simplified by choosing to monitor the applied load, which then needs to be converted into pressure by considering the device surface area. According to this, an Instron test system (model 3366) equipped with a 10 kN load cell was used. The uniaxial compression tests were performed at room temperature with two planar compression platen with a 8 cm diameter. A single load-unload cycle was performed on a representative specimen for each material. The crosshead speed was set at 0.2 mm/min. For each material, the maximum load was selected according to the outcome of preliminary tests. After those, a single set of analysis were performed on each material. For each test, the load *vs* crosshead displacement curve and the electrical capacitance and resistance signal were recorded over time. To measure the relevant electrical components, an MFIA 500 kHz Impedance Analyzer (Zurich Instruments) was interfaced with a laptop via a custom script. The device was configured to sample the impedance of the device at 10 kHz and to provide its equivalent resistance and capacitance according to the model in Figure 1.

3 RESULTS AND DISCUSSION

The mechanical and electrical behavior of the systems was evaluated by referring to the loading curves (load *vs* displacement) and the calibration curves (capacitance/resistance *vs* load), respectively. For both approaches, the hysteresis parameter, calculated as the ratio between the maximum difference on the Y-axis between the loading and unloading path, and the maximum variation on the Y-axis, was determined. Further, the single-cycle residual deformation at the very end of the unloading phase was evaluated. This means that the medium-long time viscoelastic response of the material was not taken into account at this stage. Finally, for the electrical calibration curves, an average sensitivity was estimated, considering the slope of the second line through the terminal points.

3.1 TPU

This first material that was taken into consideration (TPU) was designed as purely dielectric solid. Thus, no piezoresistive effect was expected. Thanks to previous tests, a maximum load of 900 N was applied. Considering the load-displacement curve (Figure 2), the system shows a good linear elastic response, after an initial transient region caused by imperfect specimen-plate contact. In this sample, it is possible to observe a 15.5% hysteresis between the loading and the unloading path; this phenomenon can be related to the viscoelastic nature of the material, as well as to its structure (a set of stacking layers as a result of the FDM process). The residual deformation of the system resulted in 5.4 %.
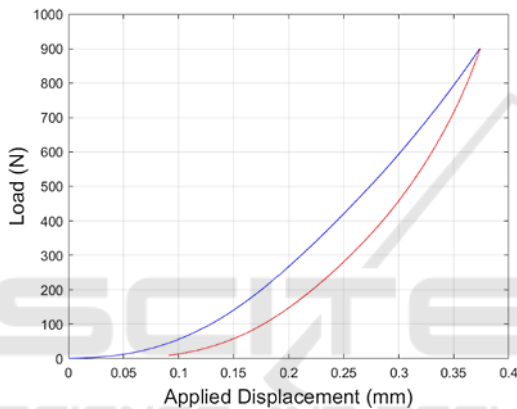

Figure 2: Load – displacement curve of TPU-based sample. The blue and red graph depict the loading and unloading respectively.

The capacitance-load curve is shown in Figure 3. It is possible to observe a general increase of the capacitance of 26.6% (2 pF), with an average sensitivity of 2.5 fF/N. A hysteresis value of 17.4%, mostly related to the mechanical properties of the dielectric material, was observed. As hinted before, the resistance variation is irrelevant and presents no correlation with the applied load (average value > 50 MΩ).

3.2 TPE

A TPE loaded with CB was studied. According to the conductive behavior of CB, it is possible to achieve a piezoresistive system since, while applying different loads, the different conductive primary particles are arranged so as to generate different conductive paths. Preliminary analyses on the material pointed out the presence of the fully-developed linear elastic region way before reaching 150 N, which was then selected
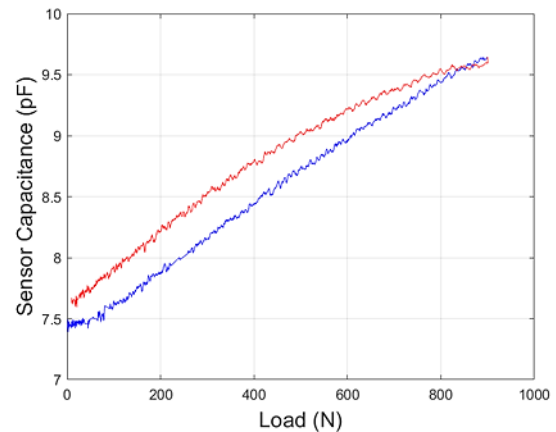

Figure 3: Capacitance – load curve of TPU-based sample. The blue and red graph depict the loading and unloading respectively.

as a threshold value for the tests. A hysteresis value of 24.5% was observed. However, the increased value concerning TPU did not result in a corresponding rise in the residual deformation, which in turn decreased to 2%. This means that 1) the hysteresis parameter cannot be considered as an indicator of the dissipative nature of the system; 2) the TPE is able to recover the strain imposed better than the TPU immediately.
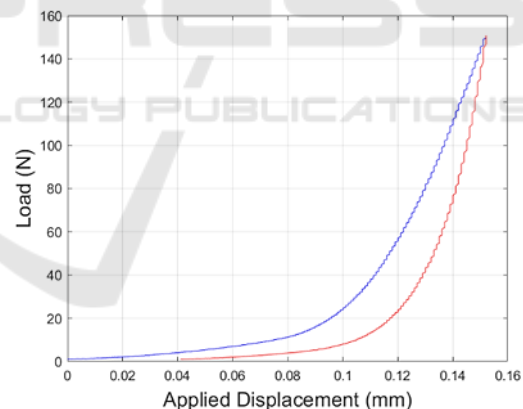

Figure 4: Load – displacement curve of TPE-based sample. The blue and red graph depict the loading and unloading respectively.

In Figure 5, the electrical behavior of the device at different loads is shown. Considering the resistance curve (Figure 5a), it is possible to observe its general and non-linear increase from approximately 300 Ω up to 900 Ω. In this frame, the device presents an average 3.8 Ω/N sensitivity that can allow only a simple measurement of the applied load. However, it should be noted that the behavior of the device is not perfectly monotone. Thus, further inquiries should be performed to gain a better understanding of the

response and to determine whether it is related to the material or the system and the experimental setup. In these conditions, it is possible to observe a hysteresis value of 26.1%. The device capacitance curve is shown in Figure 5b. The response is highly non-linear, with a non-monotone loading path. Thus, even if the capacitance ranges approximately between 180 pF and 320 pF, the possibility of developing a capacitance-based sensor is discarded, as a reliable calibration line cannot be determined. For instance, it presents hysteresis at up to 89.8%.
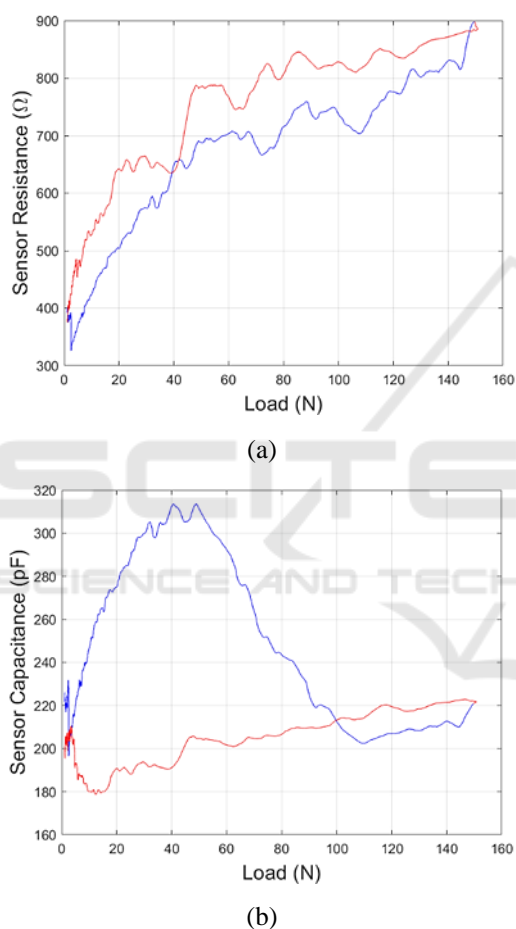

(a)

(b)

Figure 5: Resistance – load (a) and capacitance – load (b) curves of the TPE-based sample. The blue and red graphs depict the loading and unloading respectively.

3.3 SLA Resin with CB

The 1-cycle load-unload response of the SLA superflex resin with CB is shown in Figure 6. The mechanical response of the system presents some deviations from the expected trend (see TPU and TPE, for example), mainly due to the slope change at around 200N. This is supposed to be related to the

complex nature of the system, characterized by peculiar internal structuring due to the SLA technique. A hysteresis value of 21.5% was determined. The residual deformation at the end of the smooth unloading phase proved to be 2.1%. Considering electrical resistance (Figure 7a), it is possible to observe a high average value over 10 MΩ. This is related to the low (1%) loading of CB in the material that the SLA production required. However, it is possible to identify a satisfying trend that relates the output resistance to the applied load with an average sensitivity of -3.2 kΩ/N. It has to be noted that the noisy nature of the signal could have influenced the hysteresis value (42.9%). The electric capacitance (Figure 7b) stays in the range between 12.4 pF to 14.1 pF, with an average sensitivity of 1.4 fF/N. Even though this sensitivity is relevant, it must be noted that the achieved characteristics presents an hysteresis value of 38.5% and that a great part of the capacitance variation is presented at loads of less than 400 N, where the mechanical response is influenced by system-related effects. According to these observations the capacitive behavior of such device is unfit for sensing applications.
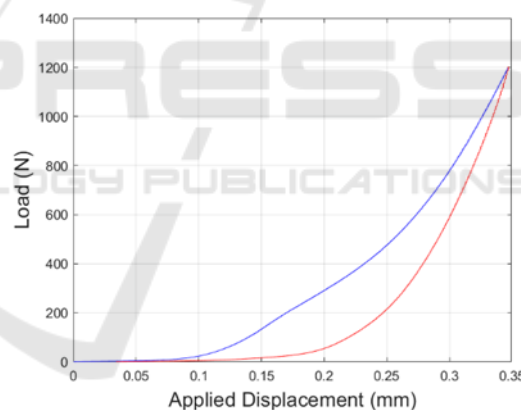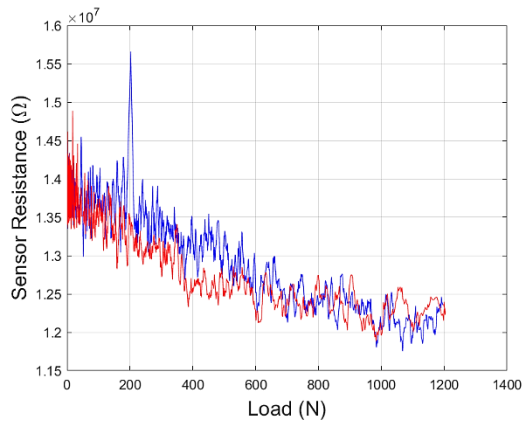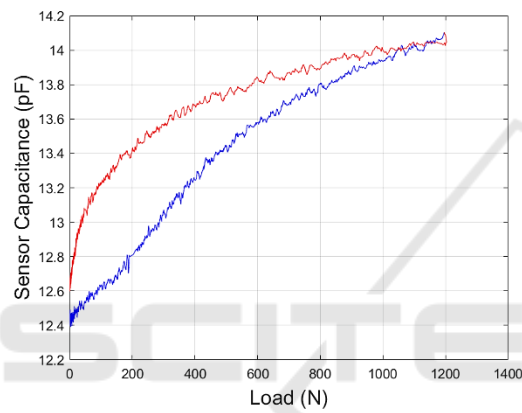

Figure 6: Load-displacement curve of the sample produced by the CB-loaded SLA resin. The blue and red graphs depict the loading and unloading respectively.

3.4 Microstructured SLA Resin

With the aim to focus on low load values (< 100 N), specific highly-compliant microstructured resin (the same type used for CB-loaded systems examined at 3.3), structures, manufactured *via* the SLA process, were studied. The mechanical response (Figure 8) is characterized by a smooth monotonic growth without any sign of discontinuity during the process. A maximum load of 90 N was applied, which was considered suitable from preliminary tests.

(a)

(b)

Figure 7: Resistance–load (a) and capacitance–load (b) curves of the sample produced by the CB-loaded SLA resin. The blue and red graphs depict the loading and unloading respectively.

Interestingly, while being deformed to higher strains (at least 3x, concerning the other materials), the unloading phase is extremely similar to its loading counterpart, leading to a small 6% hysteresis value. Further, and even more interestingly, just 0.15% of residual deformation was observed at the end of the unloading path, suggesting the possibility for it to be recovered at short times due to the viscoelastic nature of the material. This suggests the possibility for this system to be used in multi-cycle applications (at least up to 90N). The capacitance (Figure 9) is in the order of a few nF due to the reduced average relative dielectric constant produced by the air-resin blend of the dielectric. On the other hand, thanks to its flexibility and reduced stiffness, the system is characterized by a good sensitivity of 33.5 fF/N, with a reduced hysteresis of 6.2%. Thus, the possibility of fully recovering the deformation at low times and the

smooth capacitance calibration curve makes the microstructured SLA resin a promising candidate for low-load applications.
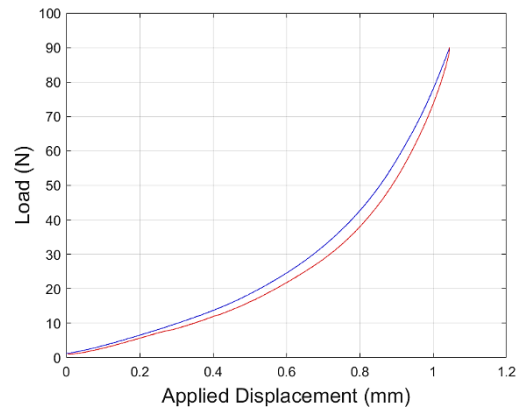

Figure 8: Load–displacement curve of the microstructured sample. The blue and red graphs depict the loading and unloading respectively.
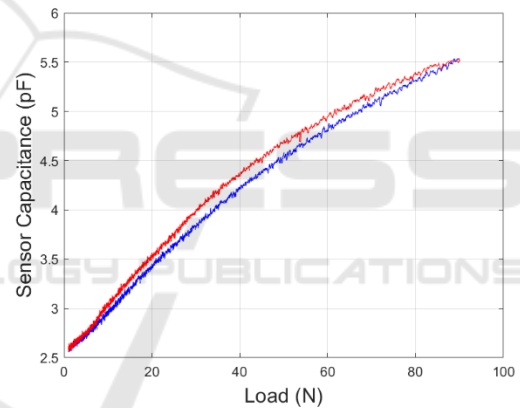

Figure 9: Capacitance–load curve of the microstructured sample. The blue and red graphs depict the loading and unloading respectively.

4 CONCLUSIONS

In this work, a set of polymeric bulk and microstructure materials were tested to inquire about their capabilities to act as transducers in pressure and force sensors. Among the possible ones, both capacitive and piezoresistive transduction principles were specifically examined. In general, it was possible to underline a hysteretic behavior on all the devices; this phenomenon is typical of polymeric structures and was observed both on the mechanical and the electrical characteristics. Interestingly, even

though the hysteresis on the capacitance of the devices has values slightly bigger (20.7% on average) than the mechanical hysteresis (16.9 % on average), the hysteresis of the resistance was generallly lower. However, it is important to notice that between each material considered, there were wide differences ranging between the mechanical hysteresis of TPE (24.5%) to one of the micro-structured devices (5.9%). Considering the maximum available load, the filled materials could withstand higher loads of up to 1200 N in general. On the other hand, the micro-structured one was less stiff and could withstand up to 90 N, with a stunning 13x increase in sensitivity concerning TPU. This outcome suggests the possibility of tuning the device stiffness and its equivalent relative dielectric constant. Considering these factors, it may be possible in future works to produce specific devices with an increased sensitivity even at low loads. Finally, the full recovery of the deformation guaranteed by the microstructured system makes it a promising candidate for multiple-cycle applications, where this requirement is mandatory. Even though some of these results are already reported in the literature, the use of fully 3D printed structures is still fairly uncommon (Sharma et al., 2022; Zong et al., 2025). It is also relevant that the achieved results in terms of sensitivity and working range seems comparable to the ones reported in the literature (Li et al., 2024; Zong et al., 2025), even though further research is needed in order to fully exploit the capabilities and flexibility of the proposed approach.

ACKNOWLEDGEMENTS

REFERENCES

Afridi, A., Al Rashid, A., & Koç, M. (2024). Recent advances in the development of stereolithography-based additive manufacturing processes: A review of applications and challenges. *Bioprinting*, *43*, e00360. https://doi.org/10.1016/j.bprint.2024.e00360

Bianchini, D., Fapanni, T., Garda, M., Leotta, F., Mecella, M., Rula, A., & Sardini, E. (2024). Digital Thread for Smart Products: A Survey on Technologies, Challenges and Opportunities in Service-Oriented Supply Chains. *IEEE Access*. https://doi.org/10.1109/ACCESS.2024.3454375

Borghetti, M., Cantu, E., Sardini, E., & Serpelloni, M. (2021). Printed Sensors for Smart Objects in Industry 4.0. *6th International Forum on Research and Technology for Society and Industry, RTSI 2021 - Proceedings*, 57–62. https://doi.org/10.1109/RTSI50628.2021.9597209

Chortos, A., Liu, J., & Bao, Z. (2016). Pursuing prosthetic electronic skin. *Nature Materials*, *15*(9), 937–950. https://doi.org/10.1038/nmat4671

El Hasnaoui, M., Triki, A., Graça, M. P. F., Achour, M. E., Costa, L. C., & Arous, M. (2012). Electrical conductivity studies on carbon black loaded ethylene butylacrylate polymer composites. *Journal of Non-Crystalline Solids*, *358*(20), 2810–2815. https://doi.org/10.1016/j.jnoncrysol.2012.07.008

Fapanni, T., Rosa, R., Cantù, E., Agazzi, F., Lopomo, N., Rosace, G., & Sardini, E. (2024). Overall Additive Manufacturing of Capacitive Sensors Integrated into Textiles: A Preliminary Analysis on Contact Pressure Estimation. *Proceedings of the 17th International Joint Conference on Biomedical Engineering Systems and Technologies*, 195–200. https://doi.org/10.5220/0012597000003657

Gao, L., Zhu, C., Li, L., Zhang, C., Liu, J., Yu, H.-D., & Huang, W. (2019). All Paper-Based Flexible and Wearable Piezoresistive Pressure Sensor. *ACS Applied Materials & Interfaces*, *11*(28), 25034–25042. https://doi.org/10.1021/acsami.9b07465

José Horst, D., & De Almeida Vieira, R. (2018). Additive Manufacturing at Industry 4.0: a Review. In *International Journal of Engineering and Technical Research* (Issue 8). www.erpublication.org

Kortuem, G., Kawsar, F., Fitton, D., & Sundramoorthy, V. (2010). *Internet of Things Track Smart Objects as Building Blocks for the Internet of Things*. www.computer.org/internet/

Laszczak, P., Jiang, L., Bader, D. L., Moser, D., & Zahedi, S. (2015). Development and validation of a 3D-printed interfacial stress sensor for prosthetic applications. *Medical Engineering & Physics*, *37*(1), 132–137. https://doi.org/10.1016/j.medengphy.2014.10.002

Li, P., Zhang, Y., Li, C., Chen, X., Gou, X., Zhou, Y., Yang, J., & Xie, L. (2024). From materials to structures: a holistic examination of achieving linearity in flexible pressure sensors. In *Nanotechnology* (Vol. 36, Issue 4). https://doi.org/10.1088/1361-6528/ad8750

Mannsfeld, S. C. B., Tee, B. C.-K., Stoltenberg, R. M., Chen, C. V. H.-H., Barman, S., Muir, B. V. O., Sokolov, A. N., Reese, C., & Bao, Z. (2010). Highly sensitive flexible pressure sensors with microstructured rubber dielectric layers. *Nature*

Materials, *9*(10), 859–864. https://doi.org/10.1038/nmat2834

Mendes, J. J. A., Vieira, M. E. M., Pires, M. B., & Stevan, S. L. (2016). Sensor fusion and smart sensor in sports and biomedical applications. In *Sensors (Switzerland)* (Vol. 16, Issue 10). MDPI AG. https://doi.org/10.3390/s16101569

Munirathinam, S. (2020). *Industry 4.0: Industrial Internet of Things (IIOT)* (pp. 129–164). https://doi.org/10.1016/bs.adcom.2019.10.010

Oh, J., Kim, D.-Y., Kim, H., Hur, O.-N., & Park, S.-H. (2022). Comparative Study of Carbon Nanotube Composites as Capacitive and Piezoresistive Pressure Sensors under Varying Conditions. *Materials*, *15*(21), 7637. https://doi.org/10.3390/ma15217637

Pan, L., Chortos, A., Yu, G., Wang, Y., Isaacson, S., Allen, R., Shi, Y., Dauskardt, R., & Bao, Z. (2014). An ultra-sensitive resistive pressure sensor based on hollow-sphere microstructure induced elasticity in conducting polymer film. *Nature Communications*, *5*. https://doi.org/10.1038/ncomms4002

Persano, L., Dagdeviren, C., Su, Y., Zhang, Y., Girardo, S., Pisignano, D., Huang, Y., & Rogers, J. A. (2013). High performance piezoelectric devices based on aligned arrays of nanofibers of poly(vinylidenefluoride-co-trifluoroethylene). *Nature Communications*, *4*. https://doi.org/10.1038/ncomms2639

Podgórski, D., Majchrzycka, K., Dąbrowska, A., Gralewicz, G., & Okrasa, M. (2017). Towards a conceptual framework of OSH risk management in smart working environments based on smart PPE, ambient intelligence and the Internet of Things technologies. *International Journal of Occupational Safety and Ergonomics*, *23*(1), 1–20. https://doi.org/10.1080/10803548.2016.1214431

Ramuz, M., Tee, B. C. K., Tok, J. B. H., & Bao, Z. (2012). Transparent, optical, pressure-sensitive artificial skin for large-area stretchable electronics. *Advanced Materials*, *24*(24), 3223–3227. https://doi.org/10.1002/adma.201200523

Saqlain, M., Piao, M., Shim, Y., & Lee, J. Y. (2019). Framework of an IoT-based Industrial Data Management for Smart Manufacturing. *Journal of Sensor and Actuator Networks*, *8*(2), 25. https://doi.org/10.3390/jsan8020025

Sharma, A., Ansari, M. Z., & Cho, C. (2022). Ultrasensitive flexible wearable pressure/strain sensors: Parameters, materials, mechanisms and applications. In *Sensors and Actuators A: Physical* (Vol. 347). Elsevier B.V. https://doi.org/10.1016/j.sna.2022.113934

Sun, L., Jiang, S., Xiao, Y., & Zhang, W. (2020). Realization of flexible pressure sensor based on conductive polymer composite via using electrical impedance tomography. *Smart Materials and Structures*, *29*(5), 055004. https://doi.org/10.1088/1361-665X/ab75a3

Wawryniuk, Z., Brancewicz-Steinmetz, E., & Sawicki, J. (2024). Revolutionizing transportation: an overview of 3D printing in aviation, automotive, and space industries. *The International Journal of Advanced Manufacturing Technology*. https://doi.org/10.1007/s00170-024-14226-y

Zong, X., Zhang, N., Ma, X., Wang, J., & Zhang, C. (2025). Polymer-based flexible piezoresistive pressure sensors based on various micro/nanostructures array. *Composites Part A: Applied Science and Manufacturing*, *190*, 108648. https://doi.org/10.1016/j.compositesa.2024.108648